Chapter 4
Universal Bells

4.1 A Brief Introduction

Most of us are familiar with several forms of bells: those in churches and cathedrals, hand-bells used in the school playground, fixed bells such as on ships and in pubs, or perhaps in hotel receptions to summon attention. Of course, there are others as we shall see. But even this short list draws attention to several *purposes* of bells, from musical instruments to information communication devices. Figure 1 provides a broad selection of bell types; you will note that they are all *suspended* with the exception of (h) which is a Japanese Zen *oryoki* which is supported on a soft cushion and struck with a hand-held mallet. The remaining group of suspended bells can be divided into two; all have the *clapper* inside the body of the bell, with the exception of (f) which is a Buddhist temple bell, *Bonsho*. Here, the almost cylindrical bell is struck by a suspended horizontal wooden pole, moved by hand.

The remaining clapper-inside bells are typical of church bells, but here there are four categories. In central Europe (a) the bell swing angle is between 60 – 70° while in the UK (b) this angle can be just over 180°. In both cases, the bell swings 'too and fro' between a positive and a negative angle. The situation in Spain (c) is completely different, where the bell angle continuously increases, the bell rotates but still the clapper is able to give periodic strikes. In all of these cases it is the *bell* that is driven by the bell ringers, and the clapper is free to work out its own motion, as we shall see. The orthodox church € has a different excitation approach; the bell is not driven, rather it is the clapper that is excited by the ringers.

The remaining two examples are (d) which is a ship's bell where the clapper is driven by hand via a short rope, and then the hand-held bell (g) where the bell is swung by hand and the clapper follows.

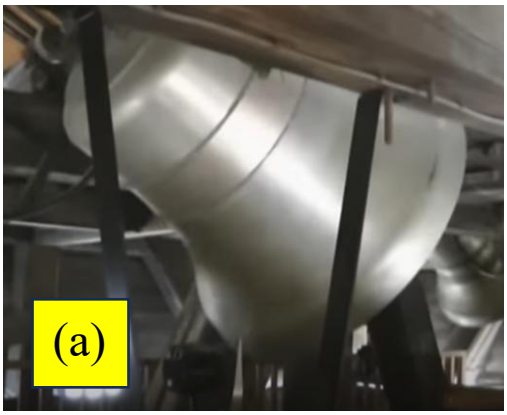
(a)

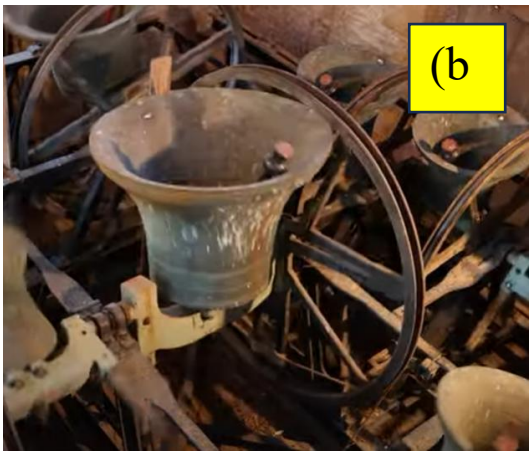
(b


(c)

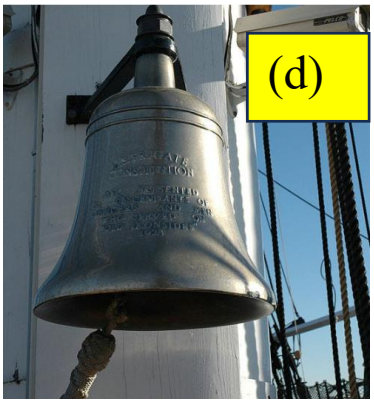
(d)


(e)


(g)


(f)


(h)

4.2 Church Bells - Equations of Motion

4.2.1 Complete Non-Linear Equations

The mechanics of the bell and clapper are shown in Fig.2(a) where pivot points are shown in yellow and M and m are masses of bell and clapper, shown at the corresponding centre of masses. The locations of the pivot points merit some discussion; the bell's pivot is often as shown, and the clapper pivot is not the same as the bell's but is located at a distance r below the bell. This is how the bell manages to exert a force on the clapper. Note that the bell angle θ is relative to the vertical, but the clapper angle φ is relative to the bell. Distance a shows the location of the bell's centre of mass relative to its pivot.

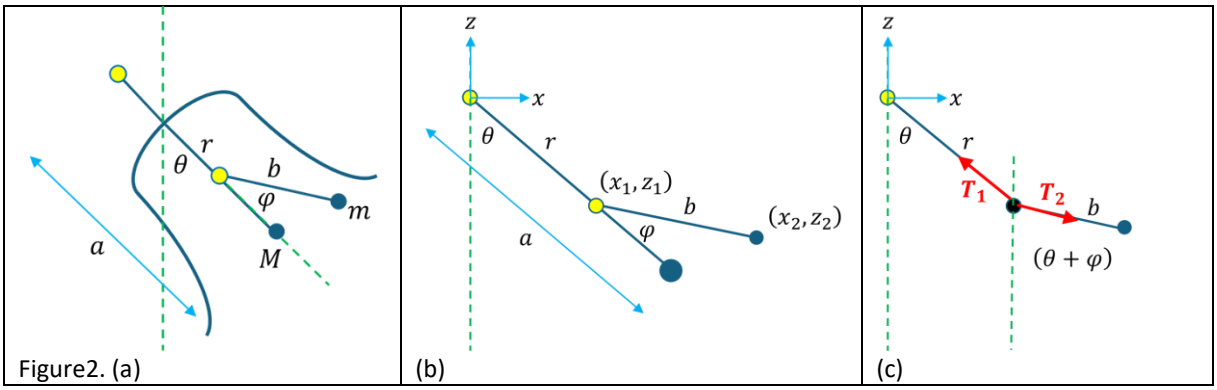

So we have here a 'double' pendulum, though it is not of the classic type where the lower pendulum is usually pivoted at the centre of mass of the upper pendulum. Fig2.(b) shows the detail. Here the clapper is rotating around its hinge located at point (x_1, z_1) which of course is *accelerating* (not just acceleration due to rotation) and so we must consider the dynamics of this point, as a precursor to the motion of (x_2, z_2). You might have noticed that we have snuck in an assumption, that the centre of mass of the clapper is located at the centre of the clapper bob. We shall see how to relax this assumption later.

Now we must consider the motion of (x_1, z_1) and (x_2, z_2). This is straightforward. We have for (x_1, z_1)

$$x_1 = r\sin\theta, \quad z_1 = -r\cos\theta$$

$$\ddot{x}_1 = r\ddot{\theta}\cos\theta - r\dot{\theta}^2\sin\theta\,, \ddot{z}_1 = r\ddot{\theta}\sin\theta - r\dot{\theta}^2\cos\theta.$$

For (x_2, z_2) we have, writing $\vartheta = \theta + \varphi$,

$$x_2 = x_1 + b\sin\vartheta\,, \qquad z_2 = z_1 - b\cos\vartheta.$$

which leads to

$$\ddot{x}_2 = \ddot{x}_1 + b\ddot{\vartheta}\cos\vartheta - b\dot{\vartheta}^2\sin\vartheta$$

$$\ddot{z}_2 = \ddot{z}_1 + b\ddot{\vartheta}\sin\vartheta + b\dot{\vartheta}^2\cos\vartheta. \qquad (1)$$

Let us hold this equation in mind and come back to use it in a moment. First, we need to consider the dynamics of the bell pendulum; the associated forces on it are shown in Fig.2(c).

$$m_1\ddot{x}_1 = T_2\sin\vartheta - T_1\sin\theta$$

$$m_2\ddot{x}_2 = T_1\cos\theta - T_2\cos\vartheta - m_1 g. \qquad (2)$$

Multiplying the first equation in this pair by $\cos\vartheta$ and the second by $\sin\vartheta$ and adding, we find

$$\ddot{x}_2\cos\vartheta + \ddot{x}_2\sin\vartheta = -g\sin\vartheta. \qquad (3)$$

So now we substitute the equations (xx) into this, replacing ϑ, and after invoking some trig identities we find

$$b\left(\ddot{\theta} + \ddot{\varphi}\right) + g\sin(\theta + \varphi) + r\ddot{\theta}\cos\varphi + r\dot{\theta}^2\sin\varphi = 0. \qquad (4)$$

We have almost reached our destination, but we need to find an expression for $\ddot{\theta}$. Here we shall make an approximation, which is quite realistic for real bells; the mass of the clapper is much less than the mass of the bell. So this allows us to *decouple* the clapper from the bell, so we assume that the bell is forced by gravity alone, and not by its connexion with the clapper. For the bell we have

$$I_B\ddot{\theta} = -Mga\sin\theta. \qquad (5)$$

We have arrived at our destination. Combining eq.4 and eq.5 and defining $l_B = I_B/Ma$ we now end up with a system of ODEs that describes our bell-clapper system

$$\ddot{\theta} = -\frac{g}{l_B}\sin\theta$$

$$\ddot{\varphi} = \frac{g}{l_B}\sin\theta - \frac{g}{b}\sin(\theta + \varphi) - \frac{r}{b}\ddot{\theta}\cos\varphi - \frac{r}{b}\dot{\theta}^2\sin\varphi. \qquad (6)$$

Of course neither the bell nor the clapper can be modelled as a mass on a massless rod; they are both physical pendulums. To take this into account, we replace l_B and b with their equivalent lengths (see Section XX) and these can be determined from the free oscillation periods of the bell and clapper.

Equation?? models the motion of bell and clapper when both are in flight; we still need to take the collisions into account. Here physics meets the details of our numerical solver. There are two possible approaches, first to model the collision as a *discrete event* and use conservation of energy and momentum to find the velocities of bell and clapper post collision. The numerical solver must be restarted using these values as new initial conditions. In the second approach we model the clapper-bell interaction *continuously* as the compression of a linear spring of large stiffness, together with an effective restitution coefficient.

4.2.2 Discussion and Alternative Derivation

The equation for the bell angular acceleration has a very familiar form; we recognize that this form originates from the gravitational force applying a torque to the bell's centre of mass.

The terms in the clapper equation look remarkably similar; the first two have gravity divided by length. The first term represents the angular acceleration of the clapper due to the bell excitation; the second term (involving length b) represents the effect of gravity acting on the clapper.

What about the two remaining terms? There is no gravity here, rather we have accelerations $r\ddot{\theta}$ and $r\dot{\theta}^2$. We recognize these as tangential components of the acceleration along a circular arc. This suggests we may be able to derive eq.6 by considering the clapper moving in a non-inertial frame provided by the bell's acceleration.

We shall use eq.6 in our simulations, but we can effect an additional simplification if we rescale time defining a new time variable $t' = t/\sqrt{l_B}$ in which case we find

$$\ddot{\theta} = -g\sin\theta$$
$$\ddot{\varphi} = g\sin\theta - g\frac{l_B}{b}\sin(\theta+\varphi) - \frac{r}{b}\ddot{\theta}\cos\varphi - \frac{r}{b}\dot{\theta}^2\sin\varphi. \quad (7)$$

The new dynamics are controlled by two non-dimensional parameters, l_B/b and r/b, so we must consider this when performing investigations.

There is one limiting situation we must consider, when $r = 0$ which means that the bell and clapper rotate around the same pivot. The bell cannot apply any torque to the clapper, until there is a collision, so the clapper will remain at rest. Remembering the definition of the clapper angle (relative to the bell), this implies that $\ddot{\varphi} = -\ddot{\theta}$ and from eq.6 we deduce that $\varphi = -\theta$ which is consistent with the clapper remaining at rest.

4.2.3 Small-angle approximation

So far, we have used the approximation $m \ll M$ which has allowed us to decouple the clapper and bell, at least the effects of the clapper on the bell which behaves like a single pendulum. Now we look for small angle solutions and make the usual trig approximations $\sin\theta \approx \theta$ and $\cos\vartheta \approx 1$. Also we can neglect terms involving nonlinear products since these will be relatively small. In other words we are now considering the system

$$\ddot{\theta} = -\frac{g}{l_B}\theta$$

$$\ddot{\varphi} = \frac{g}{l_B}\theta - \frac{g}{b}(\theta + \varphi) - \frac{r}{b}\ddot{\theta}. \quad (8)$$

With substitution of $\ddot{\theta}$ into the second equation and with a little rearrangement we have

$$\ddot{\varphi} = -\frac{g}{l_C}\varphi + g\theta\left[\frac{l_C - l_B + r}{l_C l_B}\right], \quad (9)$$

and if we take the bell's motion as $\theta = A\cos\omega_B t$ where ω_B is the bell's natural oscillation frequency, then the equation we must solve becomes

$$\ddot{\varphi} = -\frac{g}{l_C}\varphi + g\left[\frac{l_C - l_B + r}{l_C l_B}\right] A\cos\omega_B t. \quad (10)$$

This is a linear 2nd-order ODE which we can solve as a sum of homogeneous and particular solutions. But before we do that, just look at the bracket in eq.10. We see that whatever the bell's amplitude, then if $l_B = l_C + r$ then the bell will never ring, since

the angle of clapper relative to the bell will remain zero (if it starts at zero). We shall return to this soon.

Now we solve eq.10. The homogeneous solution will have the form

$$\varphi_h(t) = C_1 \cos \omega_C t + C_2 \sin \omega_C t,$$

where $\omega_C = \sqrt{g/l_C}$, the natural oscillation frequency of the clapper. For the particular solution we try

$$\varphi_p(t) = D \cos \omega t,$$

which on substitution into eq.?? yields

$$D(\omega_C^2 - \omega^2) = gA\left[\frac{l_C - l_B + r}{l_C l_B}\right].$$

So the general solution is

$$\varphi(t) = C_1 \cos \omega_C t + C_2 \sin \omega_C t + \frac{gA}{(\omega_C^2 - \omega^2)}\left[\frac{l_C - l_B + r}{l_C l_B}\right] \cos \omega t,$$

and for initial conditions $\varphi = 0,\ \dot{\varphi} = 0$ we arrive at, after a little cleaning up

$$\varphi(t) = A\frac{(l_C - l_B + r)}{(l_B - l_C)}[\cos \omega_B t - \cos \omega_C t], \qquad (11)$$

where $\omega_B = \sqrt{g/l_B}$ is the natural frequency of the bell. Note that this equation is valid only if $r \neq 0$. We can perhaps rewrite eq.11 in a more revealing way.

$$\varphi(t) = 2A\left[1 - \frac{r}{l_B - l_C}\right] \sin \tfrac{1}{2}(\omega_B + \omega_c)t \sin \tfrac{1}{2}(\omega_B - \omega_c)t. \qquad (12)$$

The constant term shows that the amplitude of φ approaches zero as *r* approaches $l_B - l_C$. The periodic terms comprise an oscillation with the average of bell and clapper frequencies modulated by half the difference in frequencies. If the bell length is close to the clapper length, then these frequencies are close, so their difference is small. Therefore the *period* of the modulation is large, and we expect our system to take a relatively long time to achieve some sort of periodic equilibrium.

4.2.4 Visualizing Bell and Clapper Rotations

First, we introduce some vocabulary. There are two ways in which the clapper may strike the bell, Fig.3.

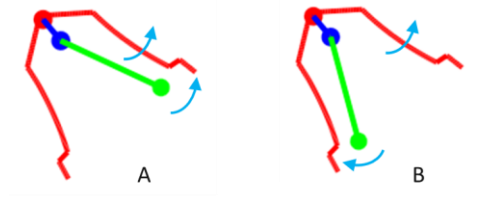

Figure 3.

In situation A the bell and clapper have the same sign of angular velocity when they collide, so the rotations are 'in-phase'. The clapper speed must be larger than the bell speed for a collision to occur, and the sign of its velocity does not change on collision. This resembles two carts on a linear air-track travelling in the same direction. This situation is known as a *flying clapper*. In situation B the bell and clapper are contra-rotating with opposite signs of angular velocity; the clapper velocity sign is inverted on collision. This is known as a *falling clapper*.

The two situations produce very different sounds; the falling clapper strike (collision) involves a large transfer of energy producing a louder sound; we refer to this strike as a *hard strike*. Conversely, the flying clapper strike involves a smaller energy transfer and a softer sound; we refer to this as a *soft strike*. Bell-ringers prefer a hard strike since they report it is easier to obtain a pleasing sound in this situation.

It may be useful to consider a hypothetical bell rotation (360°) to get the positions of bell and clapper into our heads. This is done as 10 stages in Figure 4.

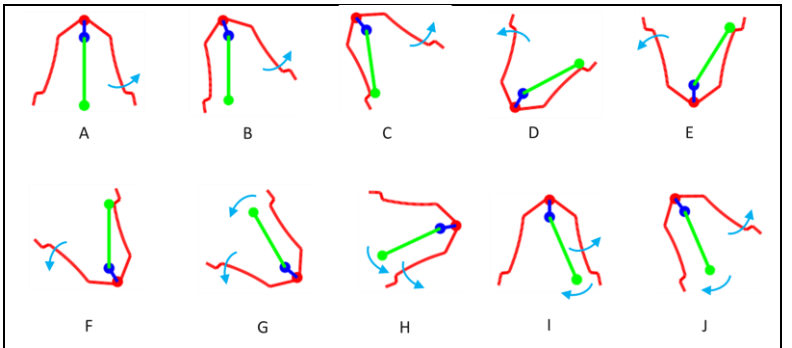

Figure 4.

Let's start with bell and clapper at rest in the vertical position, A. The bell rotates anti-clockwise, and the clapper remains at rest, B. Eventually the clapper makes contact, C, and it sticks to the bell as is dragged along with the bell, D,E,F. At F the bell has rotated beyond 180° and the clapper is vertical. At G bell and clapper have rotated a little more, so the clapper is free to rotate. The clapper rotates faster than the bell and starts to catch the bell up, H, until it strikes the bell, I, and then bounces back. Now clapper and bell are contra-rotating J. [Review this].

4.3 Great St. Mary's Cambridge Tenor Bell

We could plan investigations in a number of ways. Thinking about the parameters at our disposal, we have the ratios l_B/b and r/b which control the clapper dynamics, and of course we have the system initial conditions both for θ and φ. This opens up a potentially huge parameter space to explore, so we have to be somewhat pragmatic, and make a useful (and straightforward) choice on how to proceed.

We have decided to take a 'case study' approach, to consider some real church bells and to investigate these. The ratios l_B/b and r/b are therefore known, and all that remains is to choose our independent variable, and the initial conditions. For the independent variable we choose the *amplitude* of the bell, assuming this is constant, and make some measurement on the behaviour of the clapper. Initial conditions are, for the bell $\theta_{init} = A,\ \dot{\theta}_{init} = 0$ and for the clapper $\varphi_{init} = 0,\ \dot{\varphi}_{init} = 0$.

We shall proceed by increasing the amplitude of the bell from 0 to 180° and measuring the time intervals between successive strikes between clapper and bell, and also the number of strikes per bell swing (period).

For the first case study we have selected the Tenor bell at Great St. Mary's church, Cambridge. This bell has been selected since the required information is available[1], $l_B = 1.35m,\ L_C = 0.77m,\ r = 0.179m$. Figure5 shows simulation results bell swing angle in the range 40 – 180°. Blue dots show results of times between clapper-bell strikes, dashed lines indicate the period of the bell as a function

[1] See the journal article "The Dynamics of a Ringing Church Bell", Woodhouse et al., Advances in Acoustics and Vibration, Nov. 2012. We also express our thanks to Jim Woodhouse for personal communication.

of swing angle, together with half and one quarter period. The legend shows the different striking regimes which have emerged from the study.

Here's an overview of the results, details will be presented later. Starting from a swing of 40°, we first encounter a chaotic region where strikes occur without any definite time interval and may occur at positive or negative clapper angles without any pattern. This is followed by region 2 where there is one strike per bell swing. In region 4 there are two strikes per swing and in region 5 there are four strikes per swing. Region 3 is a transition region.

Note the green squares show the sums of individual clapper strikes over a single bell swing period, these sum to the bell period as expected.

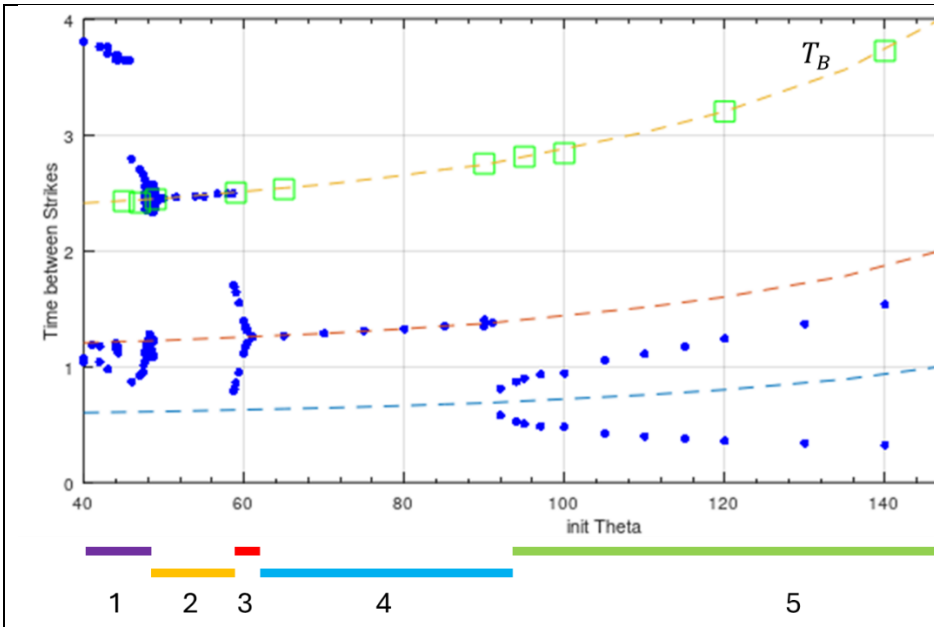

Figure 5.

This diagram is interesting and reminds us of pitchfork bifurcations, though the interpretation of the fork branches is novel as we shall see. Let's have a look at a couple of straightforward cases, for swing angle 55° and 65°.

4.3.1 Swing Angle 55°

Here we are in region 1. To understand the physics of the bell-clapper strike, we plot the bell and clapper angles, θ, φ and their angular velocities $\dot{\theta}, \dot{\varphi}$ as a function of time, see Fig.6.

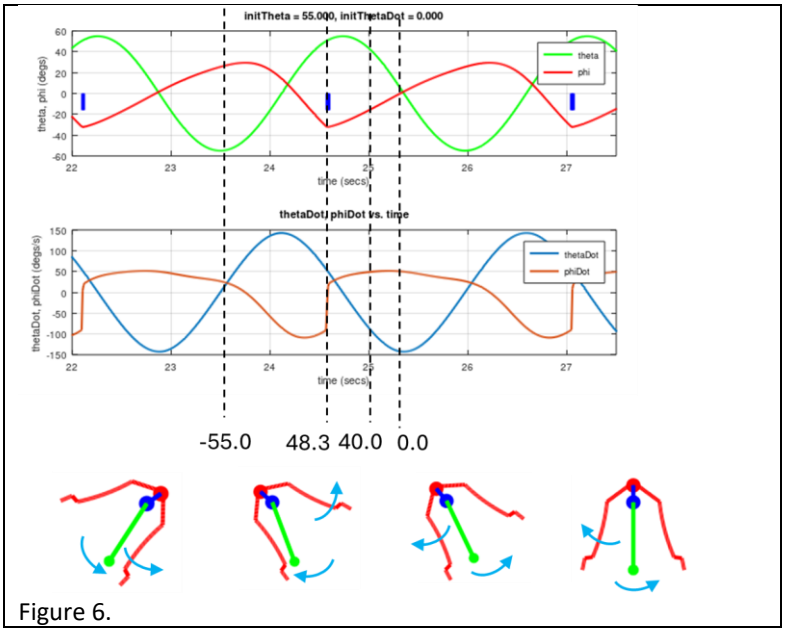

Figure 6.

Angles are shown at the top and velocities at the bottom; blue bars on the top plot shows the moment of strike. This is also clear from the abrupt change in clapper velocity. From these plots we can see at the moment of strike, at bell angle 48.3°, we have $\theta > 0$, $\dot{\theta} > 0$, $\varphi \approx -\varphi_{max}$, $\dot{\varphi} < 0$. The insets show the system at four points in its swing, to the left of vertical, at the moment of strike and later on, to the right of vertical and finally when the bell angle is zero. At -55° the clapper is rotating faster than the bell, so it is catching up which leads to the strike, and at 40° the clapper has reversed its direction of motion. As the bell continues to decrease its angle, the clapper angle increases, ready for the next cycle.

Clearly this is a falling clapper or hard strike situation. We also see that there is one strike per complete bell swing and this is exactly periodic, so we expect to hear |--------|--------|--------. (This symbolic representation indicates a strike '|' and concatenated '-' indicate the length of the time interval between strikes, here equal).

4.3.2 Swing Angle 65°

Here we are in region 4. The time traces now show two strikes per swing, Fig.8, and we have for alternate strikes

$$\theta < 0,\ \dot{\theta} < 0,\ \ \varphi \approx \varphi_{max},\ \dot{\varphi} > 0$$

$$\theta > 0,\ \dot{\theta} > 0,\ \ \varphi \approx -\varphi_{max},\ \dot{\varphi} < 0$$

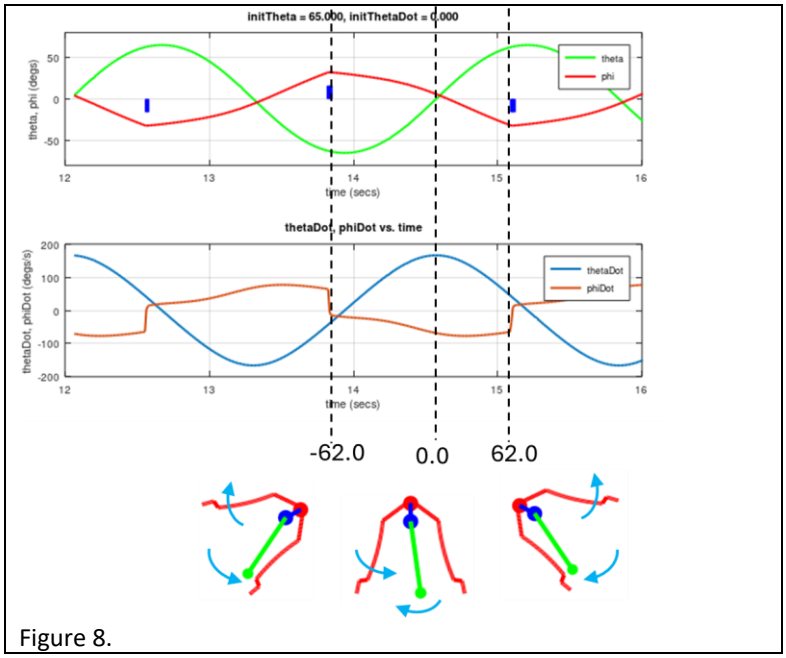

Figure 8.

The insets show the system at the first strike, when the bell passes through 0° and at the second strike. There are two strikes per complete bell swing, and we expect to hear |----|----|----; both strikes have contra-rotating bell and clapper, so they are both hard and therefore loud. The strikes are anti-symmetric; both bell and clapper angles and velocities equal and opposite. The centre inset shows when the bell is vertical, the clapper has inverted its velocity ready for the strike on the right

4.3.3 Region 3 : 58°

This transition region is bounded by the previous two examples, so we shall look at a third example in this region for a swing angle of 58°, Fig.10. The time traces have some interesting features: First we see the strikes are periodic but not regular; there is a short inter-strike interval followed by a longer one.

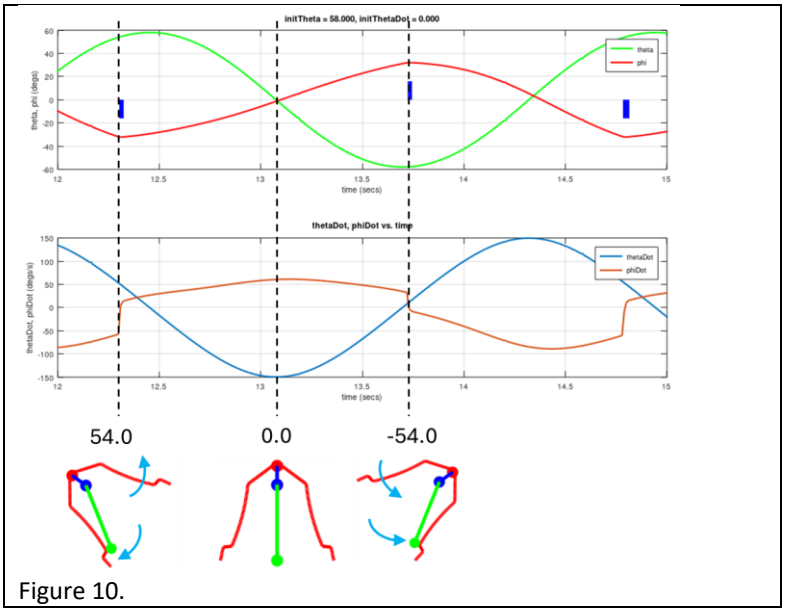

Figure 10.

The traces and inserts show we have a hard strike followed by a soft strike, so we shall hear a regular sound |--------|------|--------- where red symbols indicate a hard strike and green a soft strike. The defining difference between a hard and soft strike is visible in the change in clapper velocity on collision; for the hard strike this is larger than the soft. More energy is transferred so the sound of the hard strike is louder.

Consideration of the above time-traces yields the following states for the hard and soft rings

$$\theta > 0,\ \dot{\theta} > 0,\ \ \varphi \approx -\varphi_{max},\ \dot{\varphi} < 0 \qquad (hard)$$

$$\theta < 0,\ \dot{\theta} > 0,\ \ \varphi \approx \varphi_{max},\ \dot{\varphi} > 0 \qquad (soft)$$

The key difference is that for a hard strike the bell and clapper are contra-rotating prior to the strike, whereas for the soft strike the bell and clapper are rotating in the same direction, albeit with different speeds.

Now we can understand the changes to the system dynamics as we proceed from region 2 to region 4 through region 3. At the left of region 3 we have a single hard strike per swing, and as we enter region 3 an additional soft strike appears. Moving through region 3 this soft strike progressively becomes harder so as we exit region 3, we end up with two hard strikes per swing.

4.3.4 Region 5 : 92°

Here we move from region 4 where there are two strikes per swing into region 5 where there are (at least) four strikes per swing. Let's start by considering a swing angle of 92°, just inside region 5, time traces are shown in Fig.12

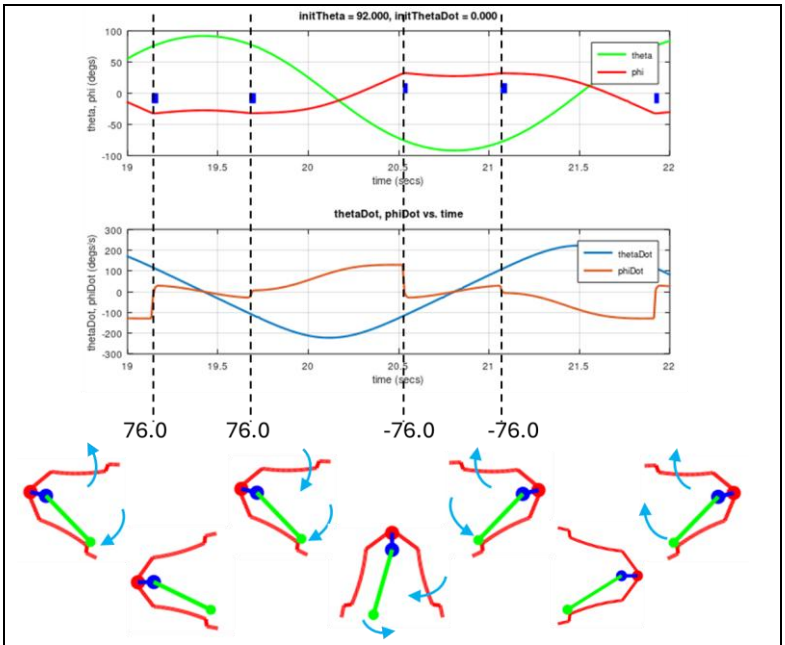

Figure 12.

There are two rows of insets; the upper row shows the system just before the strikes, and the lower row shows the bell at angle amplitude $\pm 90°$.

Compared with Fig.8 we see there is an additional strike with the sign of the bell angle unchanged. The time-trace for φ suggests the clapper bounces off the bell on the first strike, then returns to the bell to strike again. You can see this on the first three insets where the bell has a positive angle at 90° both bell and clapper velocities are essentially zero, so there must be a velocity inversion around this angle. The same argument is true for the final three insets.

We have for the two strikes at the positive bell angle:

$$\theta > 0,\ \dot{\theta} > 0,\ \ \varphi \approx -\varphi_{max},\ \dot{\varphi} < 0 \qquad (1st\ strike - hard)$$

$$\theta > 0,\ \dot{\theta} < 0,\ \ \varphi \approx -\varphi_{max},\ \dot{\varphi} < 0 \qquad (2nd\ strike - soft)$$

so the first strike is hard and the second is soft. We shall hear the following sounds: |----|------|----|------ where red strikes are loud and green are soft.

4.3.?? Region 5 : 110°

When we increase the swing to 110°, then a new phenomenon emerges; we find that following the first two strikes multiple additional strikes occur. The amplitude of these is so small that the clapper hardly moves away from the bell, these strikes will be inaudible drowned in the reverberation of the previous strikes. This situation is shown in Fig 14 which includes a magnified part of the time trace.

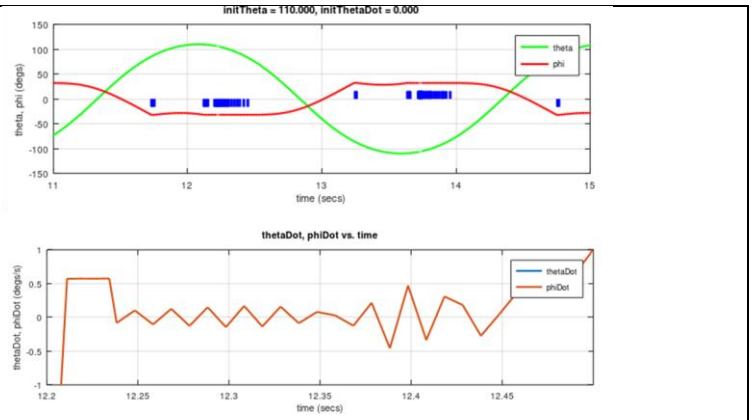

Figure 14.

4.3.?? Region 5 : 170°

Finally we move up to an angle of 170° where we see the clapper remains ‘stuck’ to the bell for a considerable time. The dynamics involves the clapper striking the bell, then following a second strike it sticks to the bell. This process happens for both halves of the bell period, see Fig.15.

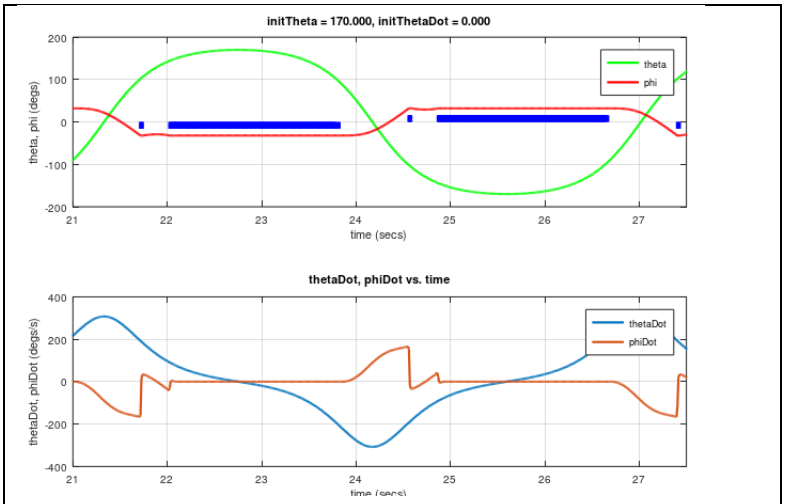

Figure 15.

4.3.5 Region 1 Chaos and Quasi-periodic behaviour

In this region we have found no periodic solutions, but there could be some lurking in a chink in the parameter space. Instead, we find chaos or regions of periodic clappering punctuated by intervals of no contact. To explore this region we measure the number of collisions per bell swing and discard the first 20 strikes to avoid any transient. This does seem rather arbitrary. The independent variable is the bell swing as usual. Results are shown in Fig.16.

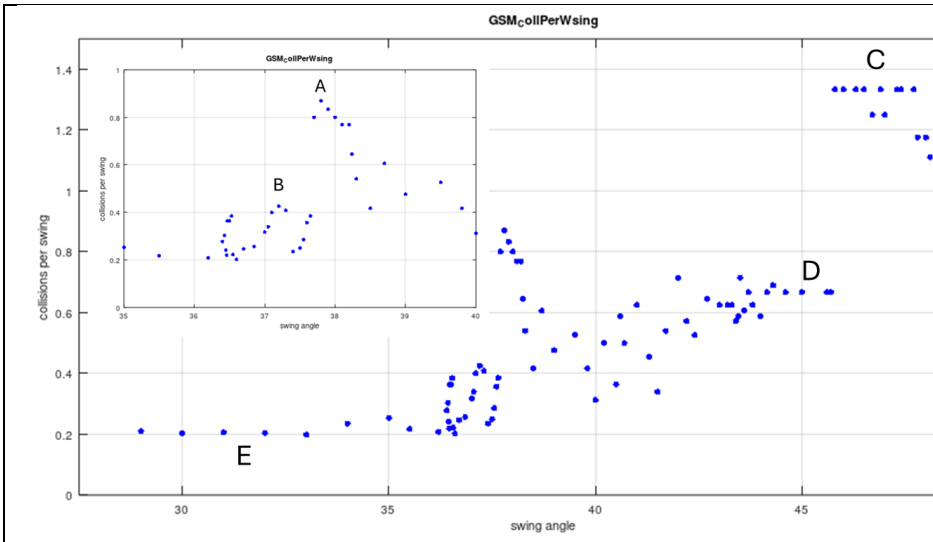

Figure 16.

As expected, the collisions per swing (cps) decreases with the swing angle, even though the swing period increases. The above plot does have a *structure*; there are three 'flat' regions and a couple of peaks. These are labelled in Fig.16 which also contains an inset of results in the range 35-40°. At A the solution consists of a mix of strikes on alternate bell sides punctuated by repeated strikea, Fig.17. This is the closest to periodic behaviour we have seen with cps just less than 1.0. At B we have more irregular

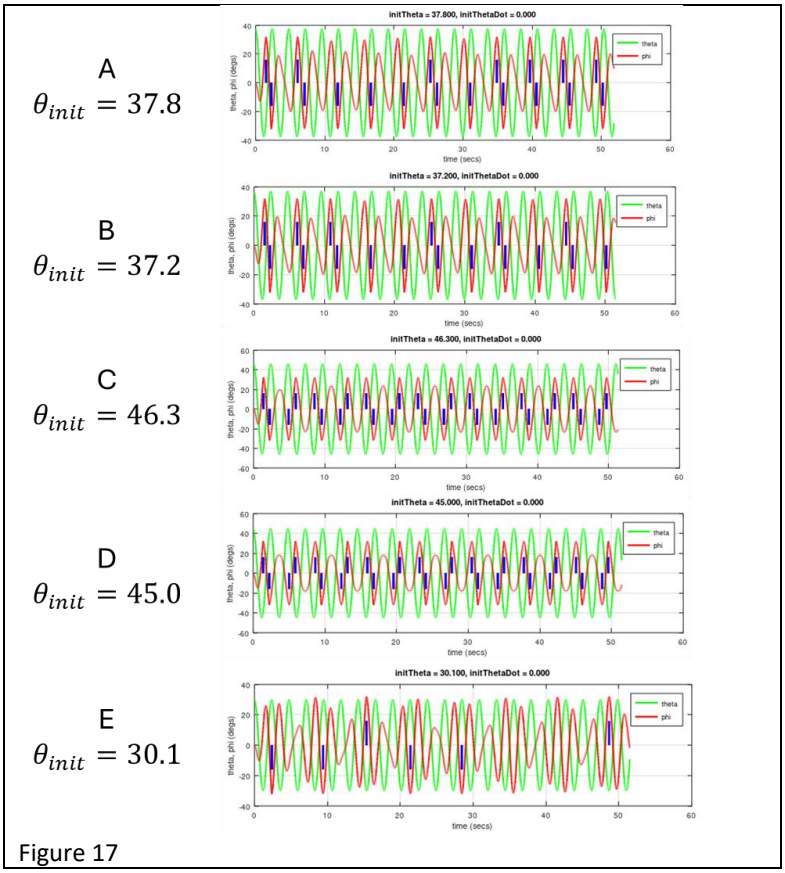

Figure 17

behaviour suggesting chaos, there are short chains of strikes on one side punctuated by one or two strikes on the other side of the bell. At C we have a periodicity of two swings and four strikes over the interval shown. At D we are looking at 2 strikes for 3 swings which agrees with the cps of 0.667. Finally at E we have another different behaviour, the time trace shows strikes punctuated by long silent intervals.

4.4 The Spanish System

Spain has a peculiar system where the bell *continually rotates* around its pivot and yet can provide regular strikes, a technique known as 'volteo'. To achieve this the bell is counterbalanced to place its centre of gravity close to the rotation axis, Fig.19, and is continuously driven by a motor through a simple belt and pulley drivetrain.

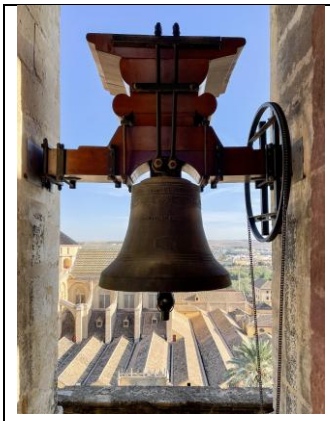

Figure 19

The governing ODEs (eq.7) can be simplified to

$$\ddot{\theta} = 0$$

$$\dot{\theta} = \Omega$$

$$\ddot{\phi} = -\frac{g}{l_C}\sin(\Omega t + \phi) - \frac{r}{l_C}\Omega^2 \sin\phi\,. \qquad (13)$$

which of course describes the dynamics between strikes. It is useful to predict possible motions of the clapper. For very low angular speeds we expect the clapper to stick to the bell following a first strike and when it has been dragged up to just past the vertical, we expect it to fall, moving faster than the bell, and strike again. For very high angular speeds we expect the clapper to experience a large centrifugal force and to have a reduced oscillationamplitude so it does not strike and there will be no sound. Between these extremes we must investigate! Results of simulations are now presented.

4.4.1 Atlas of Solutions

Here we present the results of a study of clapper motion for various bell angular speeds (°/s). There is the usual caveat that these results

may be incomplete, since it is always possible to reduce the increment in speed as we plan the simulations. Fig.20 shows an overview of various observed regimes.

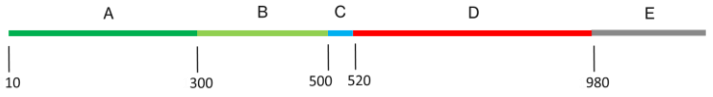

Figure 20.

In region-A we find regular patterns of strikes with significant clapper sticking; this sticking disappears in region-B which consists of regular patterns of strikes. In region-C we find packets of regular strikes separated by one or two missed strikes. Region-D shows irregular patterns of strikes, and in region-E there are no strikes.

Listening to the bell sounds we find pleasing strike patterns for $\Omega = 100, 300, 450, 500$ rev/sec, though the rate of striking for the last two speeds is too high to be useful.

Figure 21 shows time traces for a representative sample of each region. Here the green curve is the bell angle, and the red curve is the clapper angle, blue bars indicate a strike.

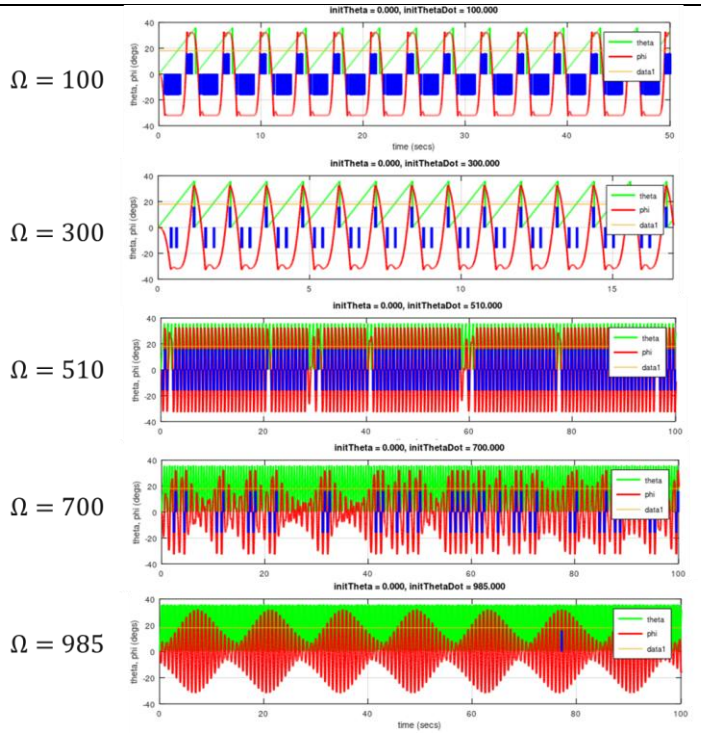

Figure 21.

Focussing on the blue bars, you can see regular behaviour for $\Omega = 100, 300$ rev/sec, with and without sticking. For $\Omega = 510$ you can see packets of regular behaviour punctuated by missed strikes. Irregular striking is observed for $\Omega = 700$, and for $\Omega = 985$ there are (almost) no strikes though an errant strike has snook in. We are close to a parameter boundary here.

Another approach to investigating different regions of bell dynamics is to plot the *time to the first strike* from a rest position where both bell and clapper are vertical. This time is indicative of the length of the initial oscillation *transient.* Results are shown in Fig.22.

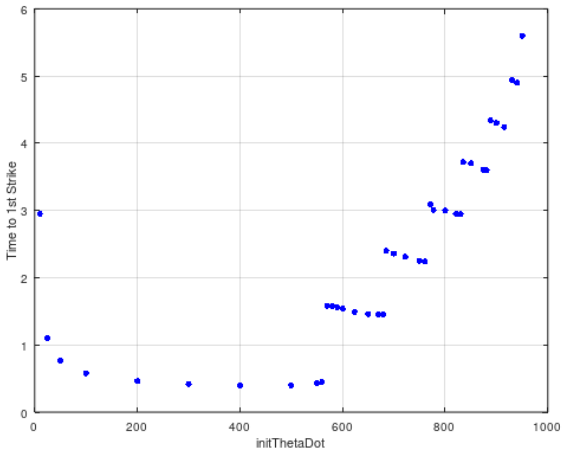

Figure 22.

As expected, the time initially decreases with rotation speed, but then almost reaches a plateau which is quite surprising. There follows a general increase separated by 'jaggies'. Investigation of these shows the clapper amplitude just misses the condition for strike, corresponding to punctuated packets of strikes. This suggests a progressive increase in length of punctuation which we do in fact observe. However a little problem emerges, Figs. 21 and 22 do not agree (we did warn that Fig.21 may be incomplete and here we find it is). Fig.22 shows that there are strikes in region-E; these were missed in the initial investigations where the simulations were stopped too soon. The results in Fig.22 do show the time to first strike is rising sharply, further investigation showed that there are no strikes for $\Omega > 990$ where the solver was run for 300 seconds.

4.4.2 Dynamics for $\Omega = 100\ °/s$

The motion of bell and clapper for a bell speed of 100°/s is shown in the time traces, Fig23. The green trace is the bell angle, red is the clapper angle and blue lines show strikes. The angular velocities of bell and clapper are also shown. Angular locations of bell and clapper are shown in the included diagrams. Starting from rest where both bell and clapper are vertical (0°) the bell rotates anti-clockwise, and the clapper strikes when the bell has reached 62°. There is a bounce and the clapper re-strikes at 76° after which it sticks to the bell. As the bell rotates further, the clapper remains stuck up to 215° (where it is just past the inverted vertical) and the clapper becomes unstuck and starts falling, rotating faster than the bell. At 276° it then strikes, rebounds and comes in to strike again at 304° followed by a small bounce and short time of sticking until it is completely free at 316°, after which the cycle repeats.

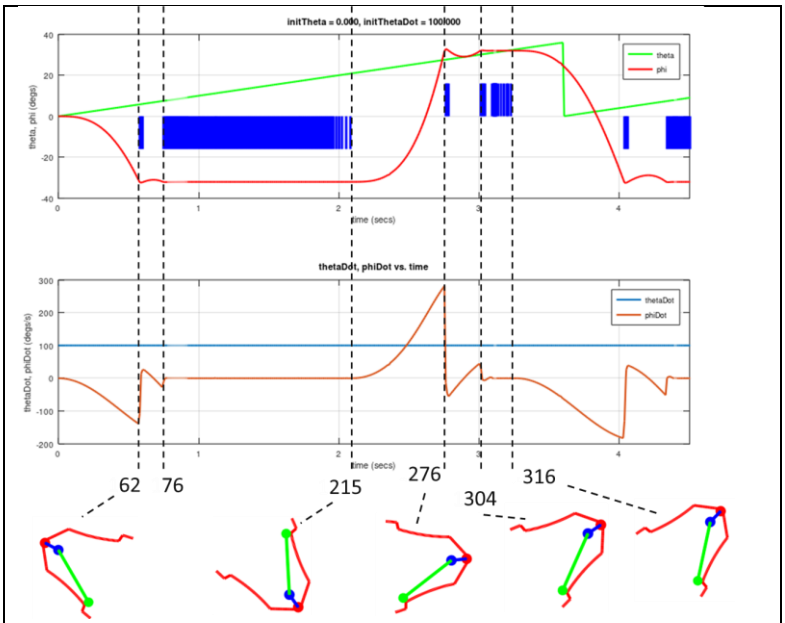

Figure 23.

So we shall hear two double strikes per bell revolution which we can write symbolically as |-|---|-|--------|-|---|-|--------. Looking at the clapper velocities at strike, we see the sounds are H-H---S-H--------. [Update above diag. w. velies.]

4.4.3 Dynamics for $\Omega = 300\ °/s$

This dynamic is more straightforward since we have no sticking. Figure 24 shows the situation; here the bell is vertical, and the

clapper has a positive angle close to the strike angle. The bell rotates faster than the clapper whose angle decreases until the bell reaches 110° where there is a falling (hard) strike. The clapper rebounds and when the bell reaches 195° there is a second hard strike. The clapper rebounds and free-falls (additional insert) until at bell angle 353° there is a third hard strike. We hear the following sequence |---|-|------|---|-|------ where all the strikes are hard.

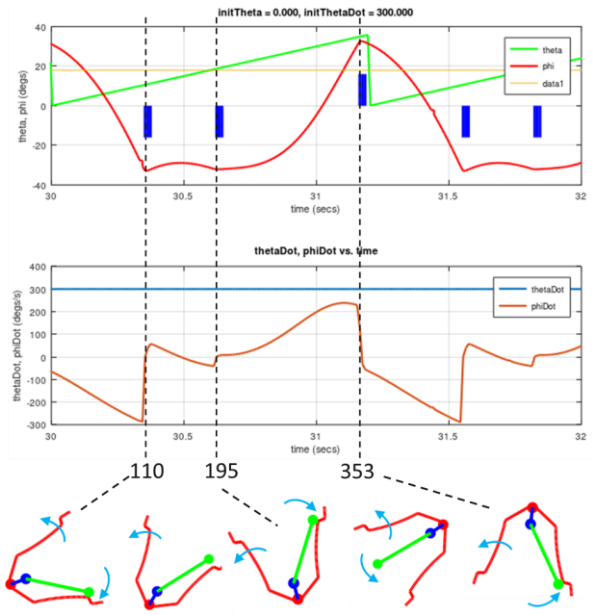

Figure 24.